Laboratory Investigation (2012) 92, 1330–1341

Distinctive contact between CD34+ hematopoietic progenitors and CXCL12+ CD271+ mesenchymal stromal cells in benign and myelodysplastic bone marrow

Eugenia Flores-Figueroa[1], Sushama Varma[2], Kelli Montgomery[2], Peter L Greenberg[3] and Dita Gratzinger[2,4]

Mesenchymal stromal cells (MSCs) support hematopoiesis and are cytogenetically and functionally abnormal in myelodysplastic syndrome (MDS), implying a possible pathophysiologic role in MDS and potential utility as a diagnostic or risk-stratifying tool. We have analyzed putative MSC markers and their relationship to CD34+ hematopoietic stem/progenitor cells (HSPCs) within intact human bone marrow in paraffin-embedded bone marrow core biopsies of benign, MDS and leukemic (AML) marrows using tissue microarrays to facilitate scanning, image analysis and quantitation. We found that CD271+, ALP+ MSCs formed an extensive branching perivascular, periosteal and parenchymal network. Nestin was brightly positive in capillary/arteriolar endothelium and occasional subendothelial cells, whereas CD146 was most brightly expressed in SMA+ vascular smooth muscle/pericytes. CD271+ MSCs were distinct by double immunofluorescence from CD163+ macrophages and were in close contact with but distinct from brightly nestin+ and from brightly CD146+ vascular elements. Double immunofluorescence revealed an intimate spatial relationship between CD34+ HSPCs and CD271+ MSCs; remarkably, 86% of CD34+ HSPCs were in direct contact with CD271+ MSCs across benign, MDS and AML marrows, predominantly in a perivascular distribution. Expression of the intercrine chemokine CXCL12 was strong in the vasculature in both benign and neoplastic marrow, but was also present in extravascular parenchymal cells, particularly in MDS specimens. We identified these parenchymal cells as MSCs by ALP/CXCL12 and CD271/CXCL12 double immunofluorescence. The area covered by CXCL12+ ALP+ MSCs was significantly greater in MDS compared with benign and AML marrow ($P = 0.021$, Kruskal–Wallis test). The preservation of direct CD271+ MSC/CD34+ HSPC contact across benign and neoplastic marrow suggests a physiologically important role for the CD271+ MSC/CD34+ HSPC relationship and possible abnormal exposure of CD34+ HSPCs to increased MSC CXCL12 expression in MDS.
Laboratory Investigation (2012) **92,** 1330–1341; doi:10.1038/labinvest.2012.93; published online 18 June 2012

KEYWORDS: bone marrow; CD271; CXCL12; mesenchymal stromal cell; microenvironment; myelodysplastic syndrome

The bone marrow microenvironment provides a crucial hematopoietic niche that promotes survival and maintenance of hematopoietic stem cells[1] and the proliferation and trilineage differentiation of CD34+ hematopoietic progenitor/stem cells (HSPCs).[2] The quantification and immunophenotyping of total CD34+ HSPCs, or blasts, is a routine component of the diagnostic bone marrow examination, and is a critical component of classification and prognostication in myelodysplastic syndrome (MDS).[3,4] In contrast, the bone marrow microenvironment remains poorly delineated in intact human marrow and is not evaluated in routine clinical practice. The bone marrow microenvironment is composed of several cell types including mesenchymal stromal cells (MSCs); prominent vasculature including specialized thin-walled sinusoids; variable numbers of adipocytes; trabecular bone and bone-lining cells; and nonmesenchymal cells, predominantly macrophages. MSCs are of particular interest because they are capable of supporting self-renewing proliferation of CD34+ hematopoietic progenitors.[5–7] Those purified MSCs that show multipotency are called

[1]Research Unit, Instituto Mexicano del Seguro Social, Mexico City, Mexico; [2]Department of Pathology, Stanford University Cancer Center, Stanford, CA, USA; [3]Hematology Division, Stanford University Cancer Center, Stanford, CA, USA and [4]Pathology Service, Veteran's Administration Palo Alto Health Care System, Palo Alto, CA, USA

Correspondence: Dr D Gratzinger, MD, PhD, Pathology Service, MC 113, VA Palo Alto Health Care System, 3801 Miranda Avenue, Palo Alto, CA 94304, USA.
E-mail: ditag@stanford.edu

Received 14 March 2012; revised 1 May 2012; accepted 15 May 2012

mesenchymal stem cells,[8] or osteoprogenitors when they demonstrate capability of reconstituting bone *in vivo*.[9] In our study we aimed to quantitatively and comprehensively map the normal MSC component of intact bone marrow to allow for identification of derangements of MSCs in myeloid neoplasia, particularly in MDS. To do so, we used markers likely to be relatively lineage specific, as single stains would be candidates for translation into the clinical laboratory setting. We have also examined the relationship of these stromal elements to CD34+ HSPCs, a population that presumably consists predominantly of CD34+ progenitors. Given the expected rarity of stem cells within the CD34+ HSPC population, our findings regarding the distribution of CD34+ HSPCs overall cannot be assumed to generically apply to the small subset of CD34+ hematopoietic stem cells, which may reside in a highly specific niche or niches.

MDS is a group of clinically and cytogenetically heterogeneous clonal bone marrow failure disorders with variable morbidity because of cytopenias and risk of transformation to acute myeloid leukemia (AML).[10] MSCs from MDS and AML patients are abnormal, demonstrating structural chromosomal abnormalities that differ from that of the hematopoietic clone and show distinct genomic profiles in cytogenetically defined or poor prognosis subgroups.[11–18] Despite this, MSCs from MDS patients are capable of supporting hematopoiesis. Recently, perturbation of mesenchymal cell populations was shown to be sufficient to induce MDS in a murine model.[19] We have mapped putative MSC markers in archival paraffin-embedded bone marrow core biopsies to ground current understanding of MSC biology within the intact human marrow in a manner that is translatable to the routine clinical laboratory setting. We have examined in detail several putative MSC markers implicated in hematopoietic stem cell niche formation in mouse models and *in vitro*, including low-affinity nerve growth factor receptor/CD271,[20] alkaline phosphatase (ALP),[21,22] nestin,[23] melanoma cell adhesion molecule/CD146[24] and the CXC chemokine CXCL12 (also termed stromal cell derived factor-1 (SDF-1)).[25] We chose the macrophage marker CD163 to provide a widely distributed nonmesenchymal comparison cell type. CD271 is expressed by a multipotent MSC population[20] and highlights ramifying stromal cells in benign and neoplastic human bone marrow.[26] Alkaline phosphatase is expressed by MSCs in culture[21] and similarly highlights reticular cells in human bone marrow.[22] Nestin, an intermediate filament protein, identifies a murine multipotent cell population capable of differentiating toward mesenchymal lineages and supporting hematopoietic stem cell homing in a mouse model.[23] Isolated CD146+ MSCs cells are able to establish the human hematopoietic microenvironment in a mouse model.[24] Finally, we examined CXCL12 expression because the so-called CXCL12-abundant reticular cells (termed CAR cells) contribute to HSPC maintenance and proliferation in mouse models;[25] CXCL12 signaling is also implicated in HSC homing and the pathophysiology of MDS in *in vitro* studies.[27–29]

Adult human bone marrow consists of parenchyma, hematopoietic elements admixed with variable amounts of fat; trabecular bone, thin layers of bone lined by predominantly quiescent osteoblasts; and vasculature.[30] Herein, we refer to zones within the bone marrow microenvironment as perivascular when they are predominantly distributed within $\sim$10–20 μm of vessels; trabecular when immediately adjacent to trabecular bone or bone-lining cells; and parenchymal when diffusely admixed with hematopoietic elements or adipocytes. These categories are not mutually exclusive as parenchyma is richly vascularized and both capillaries and sinusoids frequently occur closely apposed to trabecular bone. Sinusoids are recognized by their attenuated wall and dilated profile; capillaries are round with a small, sometimes effaced lumen and plumper endothelial cells; and arterioles have a thick profile including a plump outer layer of vascular smooth muscle and high endothelium protruding into the lumen.[31–33]

MATERIALS AND METHODS

Patient Material

Use of archival paraffin-embedded bone marrow core biopsies (BMs) and de-identified diagnostic information was approved by the institutional review board (IRB) and applicable committees at Palo Alto VA Health Care System and Stanford University School of Medicine. Requirement for individual patient consent was waived by the IRB committee. The archival BMs had been fixed in Bouin's solution (American MasterTech, Lodi, CA, USA) and decalcified (Decal solution, Decal Chemical Corporation, Tallman, NY, USA) before routine processing and embedding in paraffin. Whole BMs (12 benign, 11 MDS and 7 AML) and tissue microarrays (TMAs) composed of 1 mm cores derived from a separate set of BMs (6 benign, 5 MDS and 4 AML) were evaluated. The TMAs were constructed using a manual tissue arrayer (Beecher Instruments, Silver Spring, MD, USA). Benign biopsies were from patients being evaluated for cytopenias ($n=4$) or staged for lymphoma or solid tumors ($n=12$) who had no evidence of malignancy in their bone marrow. MDS patients across the TMA and whole core biopsies represent a range of WHO (World Health Organization)[4] diagnoses (2 refractory anemia with ring sideroblasts, 1 refractory anemia with isolated deletion 5Q, 4 refractory cytopenia with multilineage dysplasia, 3 refractory anemia with excess blasts 1 and 6 refractory anemia with excess blasts 2) and IPSS (International Prognostic Scoring System)[3] categories (2 low, 6 intermediate-1, 3 intermediate-2, and 5 high). Of the AMLs, six belonged to the WHO category of AML with myelodysplasia-related changes, and five were AML not otherwise specified. There was no statistically significant difference in the proportion of patients who had previously been exposed to chemotherapy (22%, 38% and 18% for benign, MDS and AML, respectively; χ^2 test, benign *versus* MDS, $P=0.52$; benign *versus* AML, $P=0.83$). Rare patients were currently on MDS-type therapy (eg,

lenalidomide, azacitidine) at the time of biopsy (0%, 13% and 9% for benign, MDS and AML, respectively); again, the differences were not statistically significant (χ^2 test, benign *versus* MDS, $P=0.39$; benign *versus* AML, $P=0.81$). Ages of patients were recorded in ~20-year brackets per our IRB de-identification protocol; only adult patients (≥18 years) were included. The median age bracket for benign patients was 40–59 years, whereas that for MDS and AML patients was 60–79 years, and the difference was statistically significant ($P<0.01$).

Immunohistochemistry and Immunofluorescence

Immunostaining was performed on 4-μm sections, which were placed on glass slides, baked at least 1 h at 60 °C, deparaffinized in xylene and hydrated in a graded series of alcohol. Citrate antigen retrieval (Dako, Carpinteria, CA, USA) was performed in a pressure cooker (Decloaking Chamber, Biocare Medical, Concord, CA, USA). Blocking was performed with normal donkey serum (Santa Cruz Biotechnology, Santa Cruz, CA, USA) 1:20 in phosphate-buffered saline at room temperature for 20 min. For immunohistochemistry, primary antibody staining was performed for 1 h at room temperature as indicated below. After blocking endogenous peroxidase, secondary staining was performed with horseradish peroxidase-conjugated antibodies (donkey anti-mouse, R&D, Minneapolis, MN, USA; or donkey anti-rabbit, Promega Biosystems, Sunnyvale, CA, USA) 30 min at room temperature and red chromogen (AEC, 3-amino-9-ethylcarbazole) development with the EnVision™+ Kit (Dako). For immunofluorescence, primary antibody staining was performed overnight at 4 °C as indicated below. Secondary antibody incubation (AlexaFluor488, donkey anti-mouse and Alexafluor568, donkey anti-mouse, or AlexaFluor594, goat anti-rabbit; Invitrogen, Carlsbad, CA, USA) was performed for 30 min at room temperature, after which slides were post-treated for 30 min with 0.1% Sudan Black B (Fisher Scientific, Pittsburgh, PA, USA) dissolved in 70% ethanol as described.[34] Slides were cover-slipped with Prolong Gold Antifade Reagent containing DAPI (4′,6-diamidino-2-phenylindole) nuclear counterstain (Invitrogen).

Primary Antibodies

The primary antibodies used were as follows: ALP, rabbit, 1:100 (Sigma-Aldrich, St Louis, MO, USA); CD34, mouse My10, 1:40 (BD Biosciences-Pharmingen, San Diego, CA, USA); CD31, mouse JC70A, 1:30 (Dako); CD34, rabbit, 1:40 (Abcam, Cambridge, MA, USA); CD163, rabbit, 1:100 (Lifespan Biosciences, Seattle, WA, USA); CXCL12, mouse, 1:4 (R&D); CXCR4, rabbit, 1:1000 (Novus Biologicals, Littleton, CO, USA); CD146, rabbit, 1:200 (Sigma-Aldrich); CD271, mouse, 1:100 (Invitrogen); CD271, rabbit, 1:200 (Sigma-Aldrich); Nestin, rabbit, 1:200 (Sigma-Aldrich); smooth muscle actin (SMA), mouse 1A4, 1:100 (Dako).

Image Acquisition

Light microscopic images were obtained on an Olympus BX51 upright microscope (Olympus, Center Valley, PA, USA) with UPlanFL 40×/0.75 dry or 100×/1.25 oil immersion lenses, Microfire camera and PictureFrame acquisition software (Optronics, Goleta, CA, USA). Immunofluorescence images of entire TMA cores were scanned by an Ariol dedicated scanning platform with a ×40 dry lens (UPlanFL N, 40×/0.75) and Ariol SL-50 software (Leica Microsystems, Buffalo Grove, IL, USA), CoolSNAP cf/EZ camera (Photometrics, Tucson, AZ, USA). Selected high-power widefield immunofluorescence images were taken (oil immersion) on the AxioImager 2 upright microscope with ECPlan 100×/1.3 oil immersion lens, AxioImager software and AxioCam MRm camera (Zeiss, Oberlochen, Germany); tiled images of whole cores were acquired with a PlanApoChromat 40×/0.95 dry lens and stitched together using the AxioImager software. Confocal images were obtained on the LSM 510 META platform with AxioVert 200 M inverted microscope using the PlanApoChromat 63×/1.4 oil immersion lens and the built-in image acquisition software (Zeiss).

Image Analysis

The area occupied by stromal cell populations and the distance of CD34+ hematopoietic cells to vessels and trabecular bone were assessed using ImageJ software[35] on ×40 photomicrographs of immunohistochemically stained whole or TMA BMs. Adjacency of CD34+ hematopoietic cells to stromal cell populations was manually quantitated on double-immunofluorescent-stained whole TMA core images acquired on the Ariol platform. CXCL12+/ALP+ area was quantitated in ImageJ on double-immunofluorescence-stained slides scanned on the AxioImager2 platform; after thresholding and CXCL12+ object identification, CXCL12+ objects were counted as ALP+ if at least 25% of their area was ALP+. Colocalization analysis of immunofluorescence signal in confocal images was performed using the Intensity correlation Analysis plugin in ImageJ. Statistical analysis was performed using SPSS Statistical Software 18 (IBM) as indicated in the text. Nonparametric tests were used as indicated, including Mann–Whitney test for paired independent samples, Kruskal–Wallis for multiple independent samples, Wilcoxon test for paired related samples, and Friedman test for multiple related samples.

RESULTS

CD271+ and ALP+ Are Coexpressed by a Widely Distributed Arborizing MSC Population

We analyzed the distribution of CD271 and ALP by immunohistochemistry and immunofluorescence on TMA and whole core biopsy sections. CD271+ and ALP+ cells show similar arborizing morphology, with two to three main slender projections that occasionally bifurcate. They often wrap around or closely align to adjacent structures, including trabecular bone, vessels and parenchymal components

including adipocytes, and are surrounded by mixed hematopoietic elements (representative photomicrographs, Figure 1). In the perivascular areas, CD271 and ALP+ cells show a distinctive arrangement with one cytoplasmic projection parallel to and wrapping entirely around capillaries and arterioles, and partially lining sinusoids, often with projections extending perpendicularly into the parenchyma where they are surrounded by hematopoietic elements. Given the similar morphology and distribution of the CD271 and ALP+ MSCs, we hypothesized that they represented the same population; double immunofluorescence of the entirely scanned TMA confirmed that the two populations were nearly identical (Figure 1c). ALP also rarely highlighted a separate population of CD271-negative rounded bone-lining cells consistent with osteoblasts (data not shown); where present, this population was deep to the paratrabecular layer of double positive CD271+, ALP+ stromal cells and immediately adjacent to bone. The full extent of each arborizing MSC was more completely highlighted on the membranous CD271 stain than on the ALP stain, which was cytoplasmic in distribution. The identity of CD271 and ALP+ cell populations was confirmed on confocal double-immunofluorescence-stained images with ImageJ colocalization analysis software (CD271−ALP Pearson's correlation coefficient, 0.32, mean of 9 representative images examined); the cytoplasmic (ALP) *versus* membranous (CD271) localization of the two markers accounts for incomplete colocalization within each cell.

We assessed CD163+ macrophages as a control non-mesenchymal bone marrow-resident cell population. By immunohistochemistry on the TMA the distribution of CD163+ macrophages was similar to that of CD271+ MSCs, with CD163+ macrophages scattered throughout the parenchyma and in perivascular and parosteal areas (data not shown). In fact, in paired TMA cores ($n=15$), CD163+ macrophages encompassed more than double the bone marrow area taken up by CD271+ MSCs (CD271, median area 7.0, 95% confidence interval 4.6–8.6%; CD163, median area 14.4, 95% confidence interval 11.3–15.9%; $P=0.0001$, Wilcoxon test). CD271+ MSCs and CD163+ macrophages both had multiple cytoplasmic extensions, but CD271+ cells were more elongate overall, whereas CD163+ macrophages had plumper cell bodies. By double immunofluorescence on the entirely scanned TMA, CD271+ MSCs and CD163+

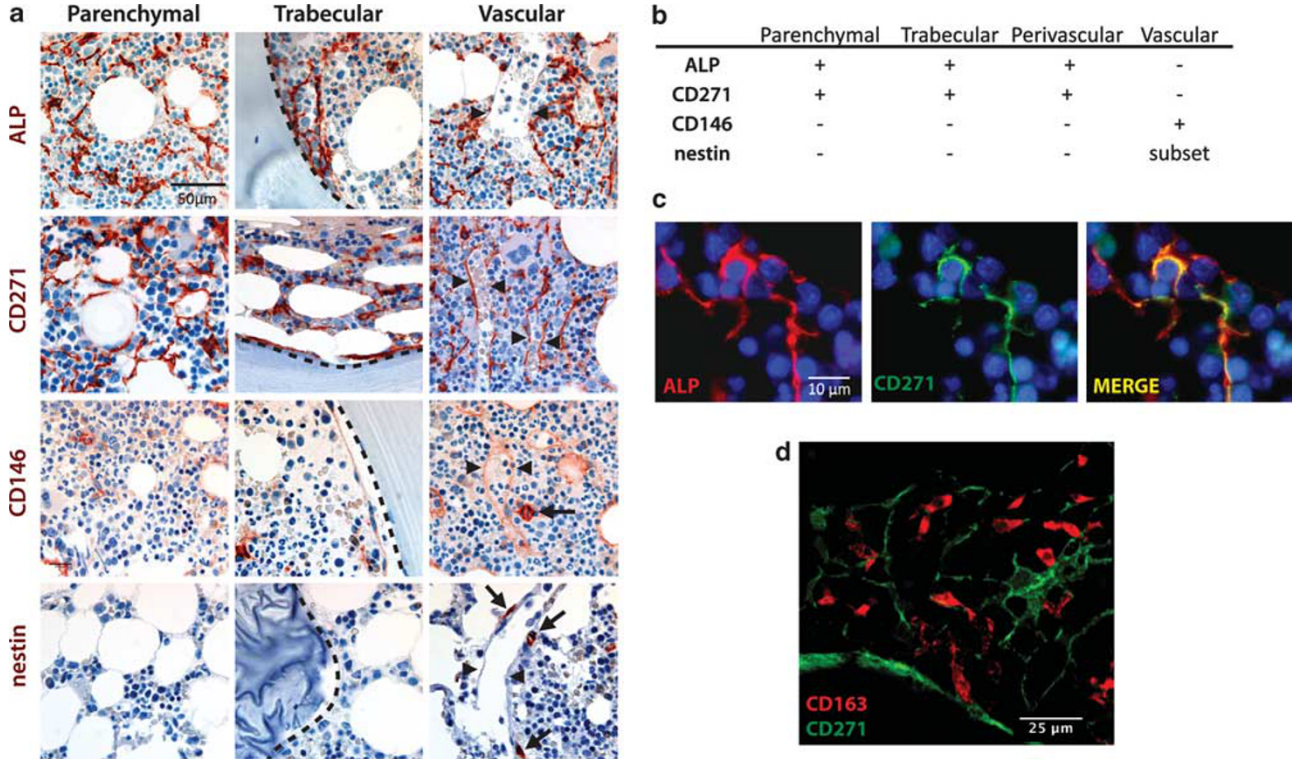

Figure 1 CD271+ and ALP (alkaline phosphatase)+ mesenchymal stromal cells (MSCs) represent the same widely distributed arborizing MSC population that predominates in a parenchymal, perivascular and paratrabecular distribution, whereas CD146 and nestin predominantly highlight vascular populations. (**a**) Representative photomicrographs of the distribution of ALP+, CD271+, CD146+ and nestin+ cells identified by immunohistochemistry (red). Trabecular bone (pale blue) is indicated by a dotted line, sinusoids by arrowheads and capillaries by arrows. (**b**) Summary of distribution of mesenchymal stromal populations within intact bone marrow. (**c**) Representative widefield photomicrographs of double immunofluorescence of CD271 and ALP demonstrate colocalization, with superimposed areas appearing yellow; the Pearson's correlation coefficient for CD271 and ALP is 0.32 based on an analysis of 9 representative confocal images at ×63. (**d**) Representative confocal photomicrograph of double immunofluorescence of CD271 and CD163 demonstrates lack of colocalization.

macrophages were two separate though intermingled populations. Representative confocal images (Figure 1d) confirmed lack of colocalization (Pearson's coefficient, −0.34, average of two × 63 images).

By immunohistochemistry and immunofluorescence, CD146 + and nestin + cell populations differed from CD271 + MSCs in both morphology and distribution. Nestin + cells were rare linear nonarborizing cells that were predominantly vascular in distribution (Figure 1). Capillaries/arterioles were strongly nestin +, whereas sinusoids were negative to dimly positive for nestin. CD146 reactivity was not cell-type specific, but strong CD146 reactivity was predominantly associated with blood vessels and was strongest in the concentric outer layers of the vessel wall in arterioles and capillaries, with dimmer CD146 reactivity present in the endothelium (Figure 1a). Adipocytes also showed variable membrane reactivity with CD146.

CD271 + and ALP + MSCs were by far the most numerous of the putative MSC populations and were greater in area than nestin + and CD146 + elements, as confirmed by quantitation of immunohistochemically positive stromal cell area in ImageJ, not including CD146 reactivity on adipocytes (Table 1). The predominantly vascular distribution of nestin + and CD146 + elements, and the partially perivascular distribution of CD271 + /ALP + MSCs, raised the question of how the three cell types interrelate spatially at the level of the marrow microvasculature.

Table 1 Quantification of percentage bone marrow area encompassed by CD271+, ALP+, CD146+ and nestin+ stromal cells

	Quantification of bone marrow areas			
	CD271	ALP	CD146	Nestin
Benign[a]	3.6 ± 3.2 (12)	7.7 ± 6.4 (12)	0.6 ± 0.9 (15)	0.0 ± 0.1 (13)
MDS	9.1 ± 8.7 (13)	10 ± 7.9 (10)	0.6 ± 0.6 (10)	0.1 ± 0.1 (10)
AML	7.1 ± 5.3 (10)	6.1 ± 7.0 (9)	0.6 ± 1.0 (10)	0.7 ± 0.2 (9)
Total	6.4 ± 6.6 (35)	8.0 ± 7.0 (31)	0.6 ± 0.8 (35)	0.1 ± 0.4 (32)
ALP[b]	1.000	—	0.001	< 0.001
CD146	0.006	0.001	—	0.60
Nestin	< 0.001	< 0.001	0.60	—
Benign *vs* MDS[c]	0.039	0.72	0.40	0.23

ALP, alkaline phosphatase; MDS, myelodysplastic syndrome; AML, acute myeloid leukemia; *vs*, *versus*.

[a]Percentage bone marrow area provided as mean ± s.d. (*n*).

[b]Friedman test *P*-value as compared with column header; adjusted for multiple comparisons.

[c]Mann–Whitney *U*-test *P*-value.

The Marrow Microvasculature Has Discrete Anatomic Compartments with Differential Relationships to CD271 + MSCs

In order to better understand the relationships among perivascular CD271 + MSCs, and the CD146, and nestin-reactive vascular elements, we performed a series of double immunofluorescence experiments on TMA sections that were scanned in widefield; confocal microscopy was also performed to confirm colocalization (representative photomicrographs, Figure 2a–f). Nestin colocalizes with CD34 in the endothelium, with strong diffuse expression in capillary/arteriolar endothelial cells as well as occasional subendothelial cells and dim/variable expression in sinusoidal endothelium (see also Figure 3c). Confirmatory co-immunofluorescence with the alternate endothelial marker CD31 confirmed coexpression of nestin by CD31 + endothelial cells (Supplementary Figure 1A). CD146 reactivity is strongest in the SMA + vascular smooth muscle/pericyte (VSMP) layer. Dimmer CD146 expression is also detectable on adipocytes and vascular endothelium, and could not be separately assessed on nestin +, CD34 − subendothelial cells. Bright CD146 expression is not noted on CD271 + or ALP + MSCs. Because of close apposition of CD271 + /ALP + MSCs to CD146 + VSMPs, adipocytes and endothelium, we cannot exclude the possibility of some partial dim membranous CD146 expression on CD271 + MSCs within the intact marrow. In arterioles/capillaries the outer layer of CD271 + MSCs is separated from the nestin + endothelium by the continuous layer of VSMP (Figure 2b–d). In contrast, sinusoidal endothelium lacks investiture with an SMA + VSMP layer but is instead in direct contact with CD271 + MSCs (Figure 2e and f; Supplementary Figure 1B and C) and, where CD271 + MSCs are lacking, sinusoidal endothelium is in direct contact with surrounding hematopoietic elements.

CD34 + HSPCs Are in Intimate Contact with CD271 + MSCs in Both Benign Bone Marrow and MDS

We next assessed the distribution of CD34 + HSPCs with respect to CD271 + MSCs, nestin bright capillary/arteriolar endothelial cells or subendothelial cells, strongly CD146 + VSMPs and CD163 + macrophages by image analysis on scanned double-immunofluorescence-stained TMA cores (quantitation and statistical analysis summarized in Table 2). The CD271/CD34 double-immunofluorescence studies reveal a remarkably intimate relationship between CD34 + HSPCs and the arborizing processes of CD271 + MSCs. The CD271 + cells are in direct contact with the HSPCs, often extending along ≥30% of their circumference, and this relationship is preserved in MDS and AML (representative images, Figure 3a). The proportion of CD34 + HSPCs adjacent to CD271 + MSCs was manually quantified, and despite the fact that only a single plane of section could be examined, on average 86 ± 8% of CD34 + HSPCs were in intimate contact with CD271 + MSCs. There was no statistically significant difference among benign, MDS and AML bone marrows with respect to the percentage of CD34 + HSPCs adjacent to CD271 + MSCs (Table 2). Only rare

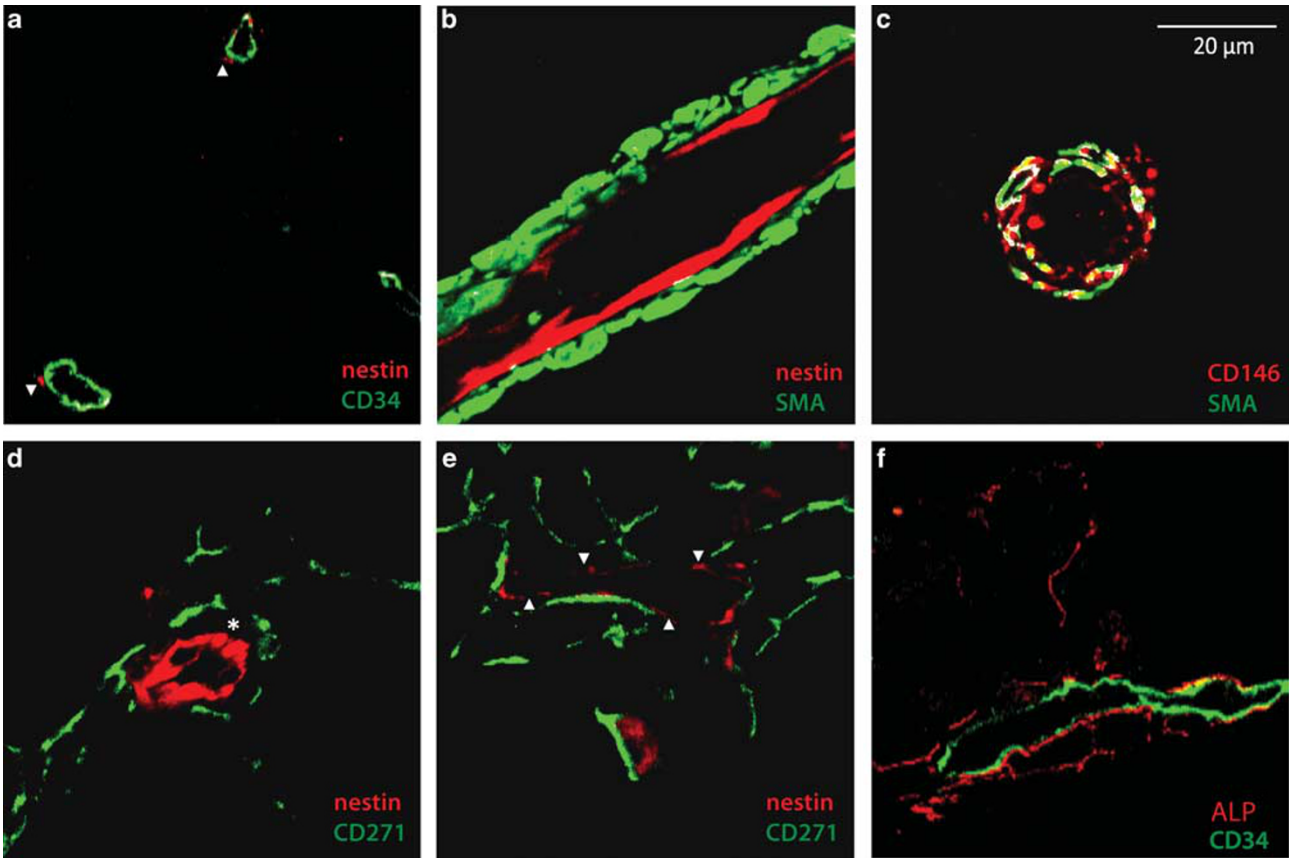

Figure 2 The marrow microvasculature has discrete anatomic compartments based on the presence of a CD146+ vascular smooth muscle/pericyte (VSMP) layer, endothelial nestin reactivity and differential contact of endothelial cells with CD271+ mesenchymal stromal cells (MSCs). Representative confocal micrographs. (**a**) Arterioles have an inner brightly nestin+, CD34+ endothelial layer (colocalization, white) and occasional nestin+ subendothelial cells (arrowheads). (**b**) Arteriolar/capillary nestin+ endothelium is surrounded by a smooth muscle actin (SMA)+ VSMP layer. (**c**) The SMA+ VSMP layer and, to a lesser extent, the plump luminal presumptive endothelial cells and possibly subendothelial cells express CD146 (red); colocalization, white. The Pearson's correlation coefficient for CD146 and SMA, based on analysis of 3 representative confocal images at ×63, is 0.24. (**d**) In arterioles, the cuff of perivascular CD271+ MSCs is separated from the nestin+ endothelium by the VSMP layer (indicated by *). (**e**, **f**) In contrast, in the gaping thin-walled sinusoids the single layer of dimly nestin+, CD34+ endothelium (indicated by arrowheads) is immediately adjacent to CD271+, ALP+ MSCs.

(<1%) CD34+ HSPCs were in contact with brightly nestin+ endothelial or subendothelial cells or brightly CD146+ VSMPs (Table 2). CD163+ macrophages encompass more than double the bone marrow area taken up by CD271+ MSCs ($P=0.0001$, Wilcoxon test), yet only 20% of HSPCs were immediately adjacent to a CD163+ macrophage. The difference among the percentage of CD34+ HSPCs in contact with CD271+ MSCs *versus* CD163+ macrophages, CD146+ VSMPs and nestin+ endothelium is statistically significant; Kruskal–Wallis test, $P<0.005$ for each of the listed pairwise comparisons after adjustment for multiple comparisons.

CD34+ HSPCs Are Perivascular in Distribution in Benign and MDS Bone Marrow

As CD271+ MSCs were present lining both trabecular bone and vessels as well as ramifying through the marrow parenchyma, we next assessed whether CD34+ HSPCs were preferentially located near vessels or trabecular bone. We quantified the distance of immunohistochemically identified CD34+ HSPCs to trabecular bone or vessels on photomicrographs from whole core biopsies (to include trabecular bone); distance to vessels was additionally assessed in TMA cores. A single cell width is between 5 and 10 μm within intact marrow; therefore, distances were binned at 10 μm intervals, with a distance within 10 μm considered to be within 1 to 2 cell widths of the relevant structure. Given that typical intertrabecular distance in the marrow in healthy adults is ~500–700 μm,[36] we limited evaluation of the distance to trabecular bone to the first 200 μm to avoid encroaching on the next trabecular zone (five ×40 fields were evaluated in each of five whole benign and MDS core biopsies).

The proportion of CD34+ HSPCs within 10 μm of a vessel was high in both benign and MDS marrow—42% in benign bone marrow and 51% in MDS—and the difference was not statistically significant (χ^2 test, $P=0.2$). In contrast, CD34+ HSPCs showed no spatial association with

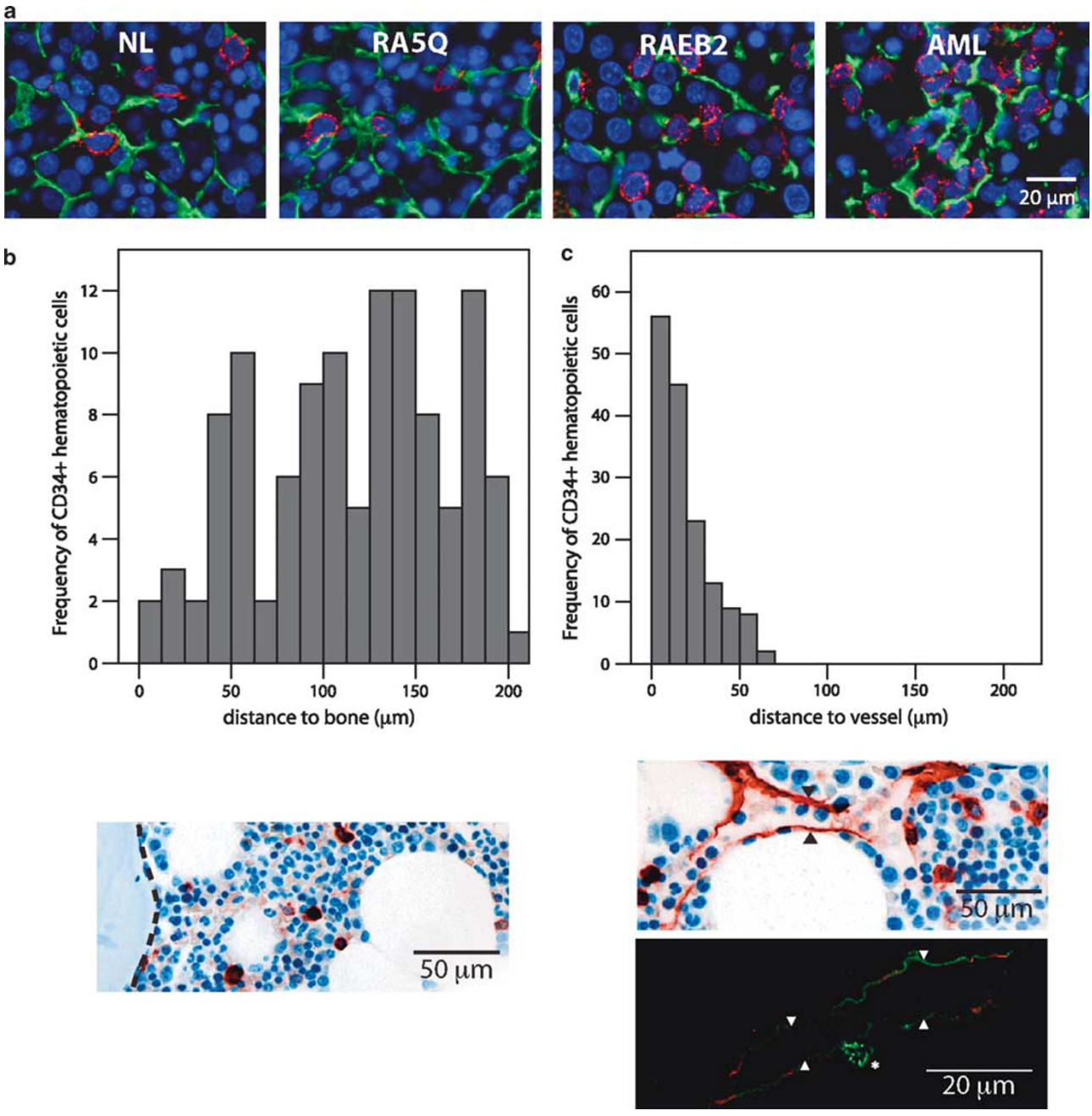

Figure 3 CD34 + HSPCs are in intimate and conserved contact with CD271 + MSCs in benign and MDS marrow and are distributed throughout the parenchyma in a perivascular pattern. (**a**) CD34 + HSPCs (red) are in intimate contact with CD271 + arborizing stromal cells (green). Representative photomicrographs of benign (NL), low-grade MDS/isolated 5Q minus (RA5Q), high-grade MDS/refractory anemia with excess blasts 2 (RAEB2) and AML bone marrow. (**b**, **c**) CD34 + HSPCs are scattered throughout the parenchyma with no preference for a periosteal location but are preferentially found near vasculature. (**b**) Histogram, distance of CD34 + HSPCs within 200 μm of trabecular bone to nearest bone surface. Representative photomicrograph demonstrating even distribution of CD34 + HSPCs (red) within bone marrow parenchyma; trabecular bone at left, indicated by dotted line. (**c**) Histogram, distance of CD34 + HSPCs to nearest vessel. Representative photomicrograph demonstrating proximity of CD34 + HSPCs to CD34 + sinusoid (indicated by arrowheads). Representative confocal image demonstrating CD34 + HSPC (asterisk) immediately adjacent to dimly nestin + /CD34 + sinusoid (indicated by arrowheads).

trabecular bone; the mean distance from CD34 + HSPCs to bone was very close to the midpoint of the area examined (Figure 3), and only a small subset of CD34 + HSPCs were found within 10 μm of bone (0.9% in benign and 2.4% in MDS marrow), with no statistically significant difference between benign and MDS (χ^2 test, $P = 0.36$). The difference in the proportion of CD34 + HSPCs within 10 μm of vessel *versus* the proportion within 10 μm of trabecular bone was highly statistically significant in both benign and MDS marrow (χ^2 test, $P < 0.0001$ in both cases).

Table 2 Quantification of CD34+ HSPCs immediately adjacent to CD271+ mesenchymal stromal cells, strongly CD146+ vascular smooth muscle/pericytes, nestin+ endothelial cells and CD163+ macrophages

	CD271	CD146	Nestin	CD163
Benign[a]	82 ± 10 (6)	0.0 ± 0.0 (5)	1.0 ± 2.1 (4)	27 ± 23 (6)
MDS	88 ± 9 (5)	0.2 ± 0.5 (5)	1.3 ± 1.6 (4)	16 ± 16 (5)
AML	88 ± 5 (4)	0.2 ± 0.3 (4)	0.5 ± 0.8 (3)	15 ± 6 (4)
Total	86 ± 7 (15)	0.1 ± 0.3 (14)	1.0 ± 0.2 (12)	20 ± 17 (15)
CD146[b]	<0.001	—	1.00	0.12
Nestin	<0.001	1.00	—	0.59
CD163	0.003	0.12	0.59	—
Benign *vs* MDS[c]	0.33	0.69	0.73	0.43

AML, acute myeloid leukemia; MDS, myelodysplastic syndrome; *vs*, *versus*.

[a]Percentage CD34+ HSPCs adjacent to each cell type provided as mean ± s.d. (*n*).

[b]Friedman test *P*-value as compared with column header; adjusted for multiple comparisons.

[c]Mann–Whitney *U*-test *P*-value.

CD271+ ALP+ MSC Area and Immunoreactivity for the Chemokine CXCL12 Are Increased in MDS

The arborizing network of CD271+ MSCs, already extensive in intact human bone marrow at baseline, appeared even denser in the parenchyma of MDS marrow. Quantitation of TMA and whole core immunohistochemical stains in ImageJ confirmed that although CD271+ MSC area was increased in MDS, there was no increase in nestin area or non-adipocytic CD146 area (Table 1). There was a near tripling of the CD271+ MSC area in MDS *versus* benign marrow, and this increase was statistically significant ($P = 0.039$; Table 1; representative photomicrographs, Figure 4a). The trend toward increased CD271+ MSC area in AML as compared with benign bone marrow was nonsignificant ($P = 0.1$, Mann–Whitney *U*-test). The increase in CD271+ MSC area in MDS was most marked in cases of low-grade MDS (defined as those with no increase in blasts, <5%). Specifically, the CD271+ MSC area in low-grade MDS was 3.6 times greater than that in benign bone marrow ($P = 0.011$, Mann–Whitney *U*-test). Nestin, CD146 and CD163 areas did not vary across diagnostic categories.

We next performed immunohistochemistry for the chemokine CXCL12 on TMA and whole core biopsies in order to assess its overall distribution. At the light microscopy level, CXCL12 expression was present in a mostly vascular distribution in benign bone marrow; in MDS and AML marrows, CXCL12 immunohistochemical reactivity was present in both a vascular and parenchymal distribution. The parenchymal CXCL12 reactivity was predominantly within elongate stromal cells, along with variable dim cytoplasmic reactivity within hematopoietic elements (and in one case bright reactivity within AML blasts). Overall, CXCL12 area by immunohistochemistry, not confined to any particular cell type, showed a nearly significant trend toward increased expression in MDS *versus* benign marrow (0.9% *vs* 3.2%, $P = 0.051$, Mann–Whitney *U*-test), whereas the comparison of benign and AML marrow was nonsignificant (0.9% *vs* 2.2%, $P = 0.2$).

The elongate CXCL12+ stromal cells showed distribution and morphology reminiscent of the CD271+ ALP+ MSC population. We performed double immunofluorescence on our TMA combining CXCL12 with CD271, ALP, CD146 and CD34, respectively, to identify the nonhematopoietic cell types producing CXCL12 (representative photomicrographs, Figure 4b–d). CXCL12 immunoreactivity was both extensive and bright in CD34+ vascular endothelium in benign, MDS and AML specimens. Extravascular stromal CXCL12 expression prominently colocalized to ALP+, CD271+ MSCs. In arterioles/capillaries, dim CXCL12 reactivity was also present in the CD146+ VSMP layer (data not shown).

Both CXCL12 and ALP showed cytoplasmic localization within CD271+ MSCs, where they would be expected to overlap; we therefore assessed for CXCL12+ elements co-localizing with ALP reactivity. We used image analysis to identify CXCL12+ cells that were also ALP+, and quantitated the area of CXCL12+/ ALP+ cells in benign, MDS and AML bone marrow. Although there was marked variability from specimen to specimen, CXCL12+/ALP+ cell area was statistically significantly increased in MDS as compared with benign and AML bone marrow, with no significant difference between the benign and AML categories (CXCL12+/ALP+ area, benign 0.3 ± 0.3%; MDS 6.9 ± 7.3%, AML 0.6 ± 0.7%; Kruskal–Wallis test, $P = 0.021$).

DISCUSSION

Systematic data regarding the intact human bone marrow microenvironment are crucial to understanding the role of abnormal MSCs in the pathophysiology of myeloid neoplasia, and to the ability to effectively evaluate these abnormalities in clinical practice. We used TMA techniques combined with semiautomated image acquisition using immunohistochemistry, double immunofluorescence and confocal microscopy to clarify the complex marrow microarchitecture and to facilitate quantification of our findings. We methodically and quantitatively analyzed the interrelationships among key components of the bone marrow microenvironment, including MSCs, macrophages, blood vessels and trabecular bone, and their relationships to CD34+ HSPCs in intact human bone marrow derived from archival diagnostic paraffin-embedded bone marrow core biopsy specimens. We characterized a CD271+, ALP+ arborizing MSC population in intact human marrow and have documented its intimate and conserved relationship to CD34+ HSPCs in both benign and myelodysplastic bone marrow. We also clarified the relationship of the bone marrow microvasculature to CD271+ MSCs, demonstrating that nestin+ CD34+ capillaries and arterioles are tightly cloaked by a SMA+,

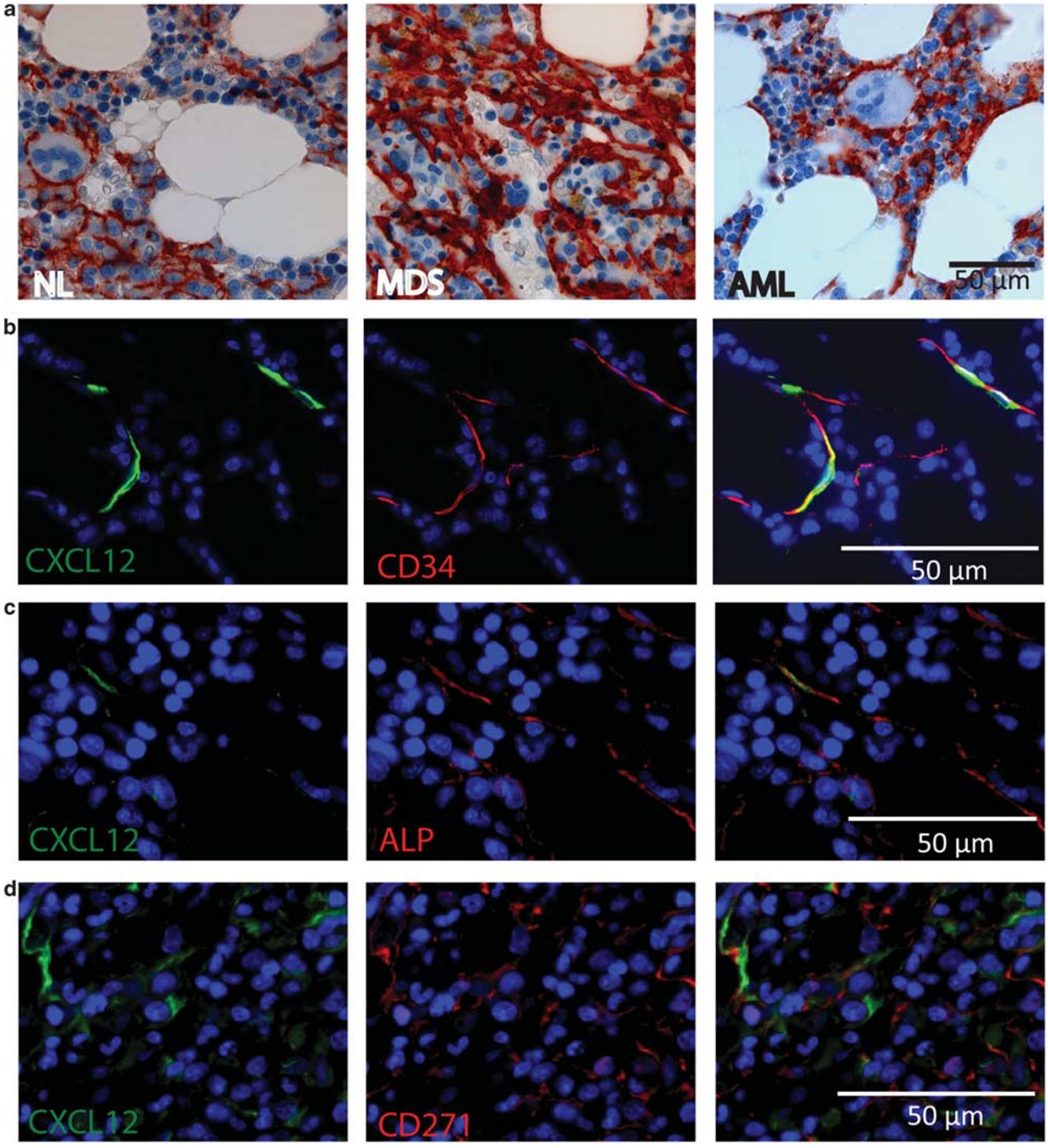

Figure 4 CD271+ mesenchymal stromal cells (MSCs) are increased in area in myelodysplastic syndrome (MDS) and express CXCL12. (**a**) The CD271+ MSC network is increased in density and extent in MDS as compared with benign (NL) and acute myeloid leukemia (AML) bone marrow (CD271, red). (**b**) Double immunofluorescence confirms CXCL12 expression within CD34+ endothelium, benign bone marrow. (**c**, **d**) Stromal CXCL12 is present within alkaline phosphatase (ALP)+ CD271+ MSCs and appears increased in MDS as compared with benign bone marrow. (**c**) Double immunofluorescence shows CXCL12 ALP coexpression within parenchymal stromal cells in benign bone marrow. (**d**) Double immunofluorescence shows CXCL12 CD271 coexpression within MDS bone marrow.

brightly CD146+ VSMP layer further surrounded by arborizing CD271+ MSCs, whereas the thin-walled, dimly nestin+ sinusoids directly contact CD271+ MSCs and hematopoietic elements. This model is in good agreement with extensive electron microscopy studies performed by Weiss[31] in the 1960s, which beautifully describe the intimate association of maturing erythroids and myeloids and platelet-budding megakaryocytes with the attenuated sinusoidal wall.

In this seminal work, Weiss[31] also describes perisinusoidal adventitial cells with rarified cytoplasm that 'extends from the sinus wall into the surrounding perisinus hematopoietic cells, separating, surrounding and loculating single cells or clusters' (p 474), a finding reminiscent of the adventitial subset of CD271+ MSCs described here. Indeed, all hematopoietic elements would be expected to be separated from the vessel endothelium by both the CD271+, ALP+ MSC layer and, depending on the site within the microvasculature, by the VSMP layer as well. CD34+ HSPCs were found predominantly within 10–20 μm of marrow microvasculature and, rarely, in direct contact with sinusoidal endothelium. As stem cells comprise a very small fraction of the CD34+ HSPC population, we cannot rule out that those rare CD34+ HSPCs that are in direct contact with nestin+ endothelial or subendothelial cells or brightly CD146+ VSMPs or that are adjacent to trabecular bone could preferentially represent hematopoietic stem cells, as suggested in some models of the hematopoietic stem cell niche.

Our data regarding the distribution of CD271+ arborizing MSCs are in agreement with excellent studies performed nearly two decades ago;[26] the intimate relationship of CD271+ arborizing MSCs to hematopoietic elements was documented by the same group using electron microscopy.[37] Proximity of CD34+ HSPCs to CD271+ MSCs was recently noted in benign human marrow,[38] in agreement with our findings. That study also demonstrated that CD146 is expressed in a subset of CD271+ MSCs of healthy donors; in our study CD146 reactivity was brightest in VSMPs, with dimmer reactivity in adipocytes and endothelium, and it is possible that any dim CD146 reactivity within CD271+ MSCs was below our threshold of detection. The difference in CD271+ MSC CD146 expression may also be partially because of differences in patient demographics between the two studies, as CD146 expression has recently been shown to decrease dramatically in older adults.[39] This group also reported detecting nestin mRNA within isolated CD271+ MSCs using 'real-time' quantitative reverse transcriptase-PCR (RQ-PCR). However, if nestin is expressed in CD271+ MSCs at the protein level, it is below the level of detection of our study and at a far lower level than nestin expression within endothelial and subendothelial cells. Endothelial nestin expression has been previously described *in vivo*, primarily in solid tumors and the brain, as well as in endothelial cell lines in culture.[40,41] Nestin expression within subendothelial cells within the vessel wall—internal to the SMA+ VSMP layer but external to the von Willebrand factor+ layer—has recently been reported;[42] we also identified occasional nestin+, CD34− subendothelial cells. The relationship between these nonendothelial nestin+ vascular wall cells and vessel wall-resident mesenchymal stem or progenitor cell populations[43] is unclear.

Human CD271+ MSCs are morphologically similar to the adventitial reticular cell population that shows mesenchymal stem cell and hematopoietic niche properties in the mouse.[9] Isolated human CD271+ MSCs have been shown to be immunophenotypically[39] and functionally[44] heterogeneous. Thus, it is entirely possible that functional subsets exist within the CD271-immunoreactive MSC population with respect to both 'niche' properties and mesenchymal stem cell properties. For example, it is possible that the subset of CD271+ MSCs present in an adventitial distribution is analogous to mouse adventitial reticular cells. In mouse, the adventitial reticular cell population is thought to be identical with the CAR cell population that has been shown to be involved in hematopoietic stem cell biology.[45,46]

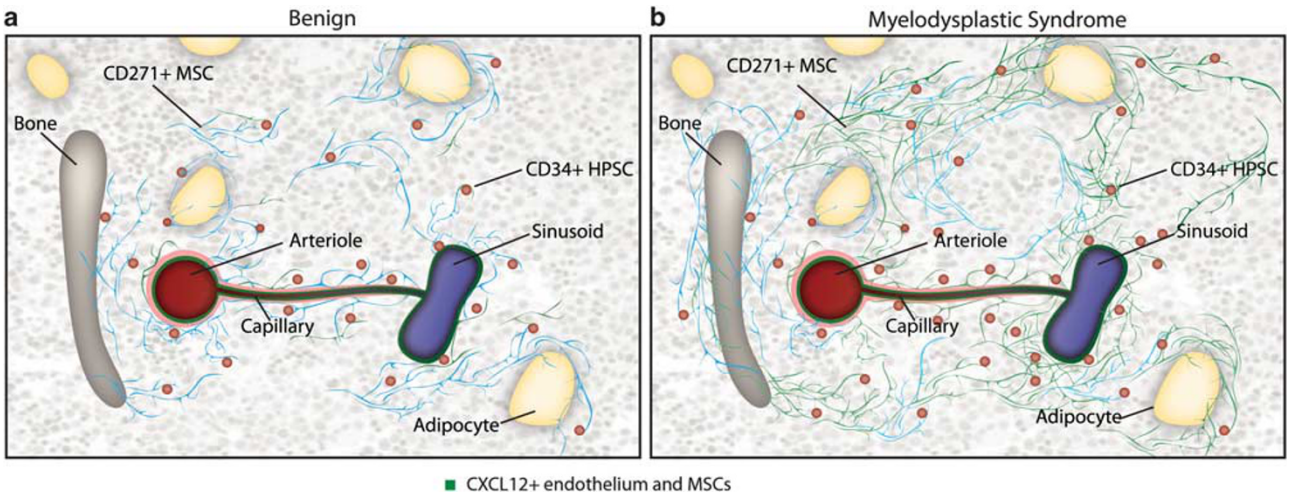

Figure 5 Model of the CD271+ mesenchymal stromal cell (MSC) niche for CD34+ hematopoietic progenitor/stem cells (HSPCs) in human bone marrow and its perturbation in myelodysplastic syndrome (MDS). (**a**) In benign bone marrow, the majority of the CD34+ HSPCs are located in intimate cell–cell contact with CD271+ MSCs. They are distributed in a perivascular pattern along the ramifying branches of perivascular CD271+ MSCs. CXCL12 expression is strong in the vasculature, and particularly the endothelium; the encircling CD271+ MSCs form a barrier between strongly CXCL12+ vascular elements and hematopoietic elements. (**b**) In MDS there is expansion of the CD271+ MSC network with increased CXCL12 expression; CD34+ HSPCs remain tightly associated with these abnormal CD271+ MSCs.

Similarly, we found that in intact human bone marrow, CD271 + ALP + MSCs were immunoreactive for CXCL12. We note that although the manufacturer raised the CXCL12 antibody against a fragment of recombinant human CXCL12, and the pattern of expression within endothelial cells and MSCs fits well with previously published studies, we have not independently confirmed the specificity of this antibody for CXCL12 within paraffin-embedded bone marrow core biopsies. It is reassuring, then, to note a recently published study[47] that demonstrated high-level CXCL12 mRNA expression in CD271 + MSCs isolated from human bone marrow aspirates. In our hands, CXCL12 intensity within CD271 + MSCs was highly variable, suggesting that these CXCL12 + MSCs may form a separate regulatable reservoir of CXCL12 within the bone marrow, in addition to CXCL12 + vascular endothelial cells. We showed a statistically significant increase in CXCL12 + /ALP + cell area in MDS as compared with benign bone marrow. CXCL12 signaling has been shown to regulate the balance between quiescence, cell cycle entry and apoptosis in CD34 + hematopoietic stem cells,[48,49] and to promote cell cycle progression in CD34 + HSPCs[50] in a contact-dependent manner *in vitro*.[7] Strong CXCL12 expression by CD271 + ALP + MSCs could be a source of abnormal survival/proliferation signaling for adjacent neoplastic CD34 + HSPCs. CXCL12 is also involved in hematopoietic stem cell homing,[27] and isolated CD34 + HSPCs from MDS patients are impaired in their ability to migrate toward CXCL12,[51] a finding that is associated with increased susceptibility to apoptosis *in vitro*.[28] Increased CXCL12 expression by MSCs could be part of a defective feedback loop between neoplastic CD34 + HSPCs and altered MSCs in MDS. The so-called 'leukemic niche'[52] may involve a spatially conserved but functionally altered relationship between the neoplastic progenitor/stem cell and its co-opted niche partners.

Based on our data we present a model for how derangements in bone marrow MSC microarchitecture and altered chemokine localization may contribute to the pathophysiology of MDS (Figure 5). We have shown that CD271 + MSCs form a network encircling sinusoids, capillaries and arteries, coating bony trabeculae and adipocytes, and ramifying through the parenchyma in intimate contact with hematopoietic elements, and in particular with CD34 + HSPCs. Bone marrow arterioles/capillaries have an inner CXCL12 + endothelial layer surrounded by an SMA + , CD146 + VSMP layer that in turn is wrapped in a layer of CD271 + MSCs that ramify into the surrounding parenchyma. Within the parenchyma, CD271 + MSC are intimately associated with hematopoietic elements including CD34 + HSPCs. In contrast, the single-layered sinusoids have CXCL12 + endothelium in direct contact with a discontinuous layer of arborizing CD271 + MSCs. CD34 + HSPCs are distributed in a perivascular manner along a network of perivascular and parenchymal arborizing CD271 + MSCs (Figure 5). As CXCL12 expression is most prominent within the vasculature in benign bone marrow, the encircling CD271 + MSCs may form a barrier between strongly CXCL12 + vascular elements and hematopoietic elements. Thus, under baseline circumstances, direct access by CD34 + HSPCs to strong contact-mediated CXCL12 signaling would be expected to be limited to exposed portions of sinusoidal endothelium. We have demonstrated that in MDS the CD271 + ALP + MSC population is expanded and shows more widespread expression of CXCL12. This more widespread MSC CXCL12 expression may expose CD34 + HSPCs to increased contact-mediated signaling with CXCL12-expressing cells. In this model the abnormal localization of immature precursors (ALIP) that has long been recognized as both a diagnostic and prognostic morphologic finding in MDS[53] might represent clusters of abnormal CD34 + HSPCs in contact with abnormal CXCL12-overexpressing CD271 + MSCs.

Supplementary Information accompanies the paper on the Laboratory Investigation website (http://www.laboratoryinvestigation.org)

ACKNOWLEDGEMENTS

This work was supported by grants from the Department of Veteran's Affairs (Biomedical Laboratory Research and Development, Career Development Award-2) and by departmental support from the Department of Pathology, Stanford University School of Medicine (to Dita Gratzinger), the Programa de Cooperación Internacional; Fondo de Investigación en Salud, Instituto Mexicano de Seguro Social; RedFarmed, Conacyt; and Agrupación Mexicana para el estudio de la Hematologia (to Eugenia Flores-Figueroa) and the William E Walsh Leukemia Research Fund (to Peter Greenberg).
The contents of this manuscript do not represent the views of the Department of Veterans Affairs, the United States Government or any other sponsoring entity.

DISCLOSURE/CONFLICT OF INTEREST

The authors declare no conflict of interest.

1. Nagasawa T, Omatsu Y, Sugiyama T. Control of hematopoietic stem cells by the bone marrow stromal niche: the role of reticular cells. Trends Immunol 2011;32:315–320.
2. Wang X, Cheng Q, Li L, *et al.* Toll-like receptors 2 and 4 mediate the capacity of mesenchymal stromal cells to support the proliferation and differentiation of $CD34^+$ cells. Exp Cell Res 2012;318:196–206.
3. Greenberg P, Cox C, LeBeau MM, *et al.* International scoring system for evaluating prognosis in myelodysplastic syndromes. Blood 1997; 89:2079–2088.
4. Swerdlow S. International Agency for Research on Cancer: World Health Organization. WHO Classification of Tumours of Haematopoietic and Lymphoid Tissues, 4th edn. International Agency for Research on Cancer: Lyon, France, 2008.
5. Muguruma Y, Yahata T, Miyatake H, *et al.* Reconstitution of the functional human hematopoietic microenvironment derived from human mesenchymal stem cells in the murine bone marrow compartment. Blood 2006;107:1878–1887.
6. Gottschling S, Saffrich R, Seckinger A, *et al.* Human mesenchymal stromal cells regulate initial self-renewing divisions of hematopoietic progenitor cells by a beta1-integrin-dependent mechanism. Stem Cells 2007;25:798–806.
7. Van Overstraeten-Schlögel N, Beguin Y, Gothot A. Role of stromal-derived factor-1 in the hematopoietic-supporting activity of human mesenchymal stem cells. Eur J Haematol 2006;76:488–493.
8. Pittenger MF, Mackay AM, Beck SC, *et al.* Multilineage potential of adult human mesenchymal stem cells. Science 1999;284:143–147.
9. Bianco P. Bone and the hematopoietic niche: a tale of two stem cells. Blood 2011;117:5281–5288.

10. Greenberg PL. Current therapeutic approaches for patients with myelodysplastic syndromes. Br J Haematol 2010;150:131–143.
11. Tauro S, Hepburn MD, Bowen DT, *et al.* Assessment of stromal function, and its potential contribution to deregulation of hematopoiesis in the myelodysplastic syndromes. Haematologica 2001;86:1038–1045.
12. Flores-Figueroa E, Gutierrez-Espindola G, Montesinos JJ, *et al.* In vitro characterization of hematopoietic microenvironment cells from patients with myelodysplastic syndrome. Leuk Res 2002;26:677–686.
13. Kitagawa M, Saito I, Kuwata T, *et al.* Overexpression of tumor necrosis factor (TNF)-alpha and interferon (IFN)-gamma by bone marrow cells from patients with myelodysplastic syndromes. Leukemia 1997;11:2049–2054.
14. Ohmori S, Ohmori M, Yamagishi M, *et al.* MDS-macrophage derived inhibitory activity on myelopoiesis of MDS abnormal clones. Br J Haematol 1993;83:388–391.
15. Flores-Figueroa E, Arana-Trejo RM, Gutierrez-Espindola G, *et al.* Mesenchymal stem cells in myelodysplastic syndromes: phenotypic and cytogenetic characterization. Leuk Res 2005;29:215–224.
16. Blau O, Hofmann WK, Baldus CD, *et al.* Chromosomal aberrations in bone marrow mesenchymal stroma cells from patients with myelodysplastic syndrome and acute myeloblastic leukemia. Exp Hematol 2007;35:221–229.
17. Lopez-Villar O, Garcia JL, Sanchez-Guijo FM, *et al.* Both expanded and uncultured mesenchymal stem cells from MDS patients are genomically abnormal, showing a specific genetic profile for the 5q- syndrome. Leukemia 2009;23:664–672.
18. Blau O, Baldus CD, Hofmann W-K, *et al.* Mesenchymal stromal cells of myelodysplastic syndrome and acute myeloid leukemia patients have distinct genetic abnormalities compared with leukemic blasts. Blood 2011;118:5583–5592.
19. Raaijmakers MH, Mukherjee S, Guo S, *et al.* Bone progenitor dysfunction induces myelodysplasia and secondary leukaemia. Nature 2010;464:852–857.
20. Quirici N, Soligo D, Bossolasco P, *et al.* Isolation of bone marrow mesenchymal stem cells by anti-nerve growth factor receptor antibodies. Exp Hematol 2002;30:783–791.
21. Conrad C, Zeindl-Eberhart E, Moosmann S, *et al.* Alkaline phosphatase, glutathione-S-transferase-P, and cofilin-1 distinguish multipotent mesenchymal stromal cell lines derived from the bone marrow versus peripheral blood. Stem Cells Dev 2008;17:23–27.
22. Westen H, Bainton DF. Association of alkaline-phosphatase-positive reticulum cells in bone marrow with granulocytic precursors. J Exp Med 1979;150:919–937.
23. Mendez-Ferrer S, Michurina TV, Ferraro F, *et al.* Mesenchymal and haematopoietic stem cells form a unique bone marrow niche. Nature 2010;466:829–834.
24. Sacchetti B, Funari A, Michienzi S, *et al.* Self-renewing osteoprogenitors in bone marrow sinusoids can organize a hematopoietic microenvironment. Cell 2007;131:324–336.
25. Omatsu Y, Sugiyama T, Kohara H, *et al.* The essential functions of adipo-osteogenic progenitors as the hematopoietic stem and progenitor cell niche. Immunity 2010;33:387–399.
26. Cattoretti G, Schiro R, Orazi A, *et al.* Bone marrow stroma in humans: anti-nerve growth factor receptor antibodies selectively stain reticular cells in vivo and in vitro. Blood 1993;81:1726–1738.
27. Sharma M, Afrin F, Satija N, *et al.* Stromal-derived factor-1/CXCR4 signaling: indispensable role in homing and engraftment of hematopoietic stem cells in bone marrow. Stem Cells Dev 2011;20:933–946.
28. Matsuda M, Morita Y, Hanamoto H, *et al.* CD34+ progenitors from MDS patients are unresponsive to SDF-1, despite high levels of SDF-1 in bone marrow plasma. Leukemia 2004;18:1038–1040.
29. Yang R, Pu J, Guo J, *et al.* The biological behavior of SDF-1/CXCR4 in patients with myelodysplastic syndrome. Med Oncol 2011.
30. Brown DC, Gatter KC. The bone marrow trephine biopsy: a review of normal histology. Histopathology 1993;22:411–422.
31. Weiss L. The structure of bone marrow. Functional interrelationships of vascular and hematopoietic compartments in experimental hemolytic anemia: an electron microscopic study. J Morphol 1965;117:467–537.
32. Burkhardt R, Kettner G, Böhm W, *et al.* Changes in trabecular bone, hematopoiesis and bone marrow vessels in aplastic anemia, primary osteoporosis, and old age: a comparative histomorphometric study. Bone 1987;8:157–164.
33. Thiele J, Rompcik V, Wagner S, *et al.* Vascular architecture and collagen type IV in primary myelofibrosis and polycythaemia vera: an immunomorphometric study on trephine biopsies of the bone marrow. Br J Haematol 1992;80:227–234.
34. Baschong W, Suetterlin R, Laeng RH. Control of autofluorescence of archival formaldehyde-fixed, paraffin-embedded tissue in confocal laser scanning microscopy (CLSM). J Histochem Cytochem 2001;49:1565–1572.
35. Collins TJ. ImageJ for microscopy. BioTechniques 2007;43(1 Suppl):25–30.
36. Christiansen P, Steiniche T, Vesterby A, *et al.* Primary hyperparathyroidism: iliac crest trabecular bone volume, structure, remodeling, and balance evaluated by histomorphometric methods. Bone 1992;13:41–49.
37. Caneva L, Soligo D, Cattoretti G, *et al.* Immuno-electron microscopy characterization of human bone marrow stromal cells with anti-NGFR antibodies. Blood Cells Mol Dis 1995;21:73–85.
38. Tormin A, Li O, Brune JC, *et al.* CD146 expression on primary nonhematopoietic bone marrow stem cells is correlated with in situ localization. Blood 2011;117:5067–5077.
39. Maijenburg MW, Kleijer M, Vermeul K, *et al.* The composition of the mesenchymal stromal cell compartment in human bone marrow changes during development and aging. Haematologica 2011;97:179–183.
40. Sugawara K, Kurihara H, Negishi M, *et al.* Nestin as a marker for proliferative endothelium in gliomas. Lab Invest 2002;82:345–351.
41. Aihara M, Sugawara K, Torii S, *et al.* Angiogenic endothelium-specific nestin expression is enhanced by the first intron of the nestin gene. Lab Invest 2004;84:1581–1592.
42. Ferraro F, Lymperi S, Méndez-Ferrer S, *et al.* Diabetes impairs hematopoietic stem cell mobilization by altering niche function. Sci Transl Med 2011;3(104):104ra101.
43. Corselli M, Chen C-W, Crisan M, *et al.* Perivascular ancestors of adult multipotent stem cells. Arterioscler Thromb Vasc Biol 2010;30:1104–1109.
44. Battula VL, Treml S, Bareiss PM, *et al.* Isolation of functionally distinct mesenchymal stem cell subsets using antibodies against CD56, CD271, and mesenchymal stem cell antigen-1. Haematologica 2009;94:173–184.
45. Sugiyama T, Kohara H, Noda M, *et al.* Maintenance of the hematopoietic stem cell pool by CXCL12-CXCR4 chemokine signaling in bone marrow stromal cell niches. Immunity 2006;25:977–988.
46. Askmyr M, Sims NA, Martin TJ, *et al.* What is the true nature of the osteoblastic hematopoietic stem cell niche? Trends Endocrinol Metab 2009;20:303–309.
47. Churchman SM, Ponchel F, Boxall SA, *et al.* Native CD271(+) multipotential stromal cells (MSCs) have a transcript profile indicative of multiple fates with prominent osteogenic and Wnt pathway signalling activity. Arthritis Rheum 2012, Available at http://www.ncbi.nlm.nih.gov/pubmed/22378497.
48. Lataillade JJ, Clay D, Dupuy C, *et al.* Chemokine SDF-1 enhances circulating CD34(+) cell proliferation in synergy with cytokines: possible role in progenitor survival. Blood 2000;95:756–768.
49. Lataillade J-J, Clay D, Bourin P, *et al.* Stromal cell-derived factor 1 regulates primitive hematopoiesis by suppressing apoptosis and by promoting G(0)/G(1) transition in CD34(+) cells: evidence for an autocrine/paracrine mechanism. Blood 2002;99:1117–1129.
50. Chabanon A, Desterke C, Rodenburger E, *et al.* A cross-talk between stromal cell-derived factor-1 and transforming growth factor-beta controls the quiescence/cycling switch of CD34(+) progenitors through FoxO3 and mammalian target of rapamycin. Stem Cells 2008;26:3150–3161.
51. Fuhler GM, Drayer AL, Olthof SGM, *et al.* Reduced activation of protein kinase B, Rac, and F-actin polymerization contributes to an impairment of stromal cell derived factor-1 induced migration of CD34+ cells from patients with myelodysplasia. Blood 2008;111:359–368.
52. Lane SW, Scadden DT, Gilliland DG. The leukemic stem cell niche: current concepts and therapeutic opportunities. Blood 2009;114:1150–1157.
53. Verburgh E, Achten R, Maes B, *et al.* Additional prognostic value of bone marrow histology in patients subclassified according to the International Prognostic Scoring System for myelodysplastic syndromes. J Clin Oncol 2003;21:273–282.